Ground-state correlations and final state interactions in the process $^3\text{He}(e,e'pp)n$

C. Ciofi degli Atti and L. P. Kaptari*

Department of Physics, University of Perugia, and INFN, Sezione di Perugia, via A. Pascoli, Perugia, I-06100, Italy
(Received 5 May 2002; published 17 October 2002)

The two-proton emission process $^3\text{He}(e,e'pp)n$ is theoretically investigated using realistic three-nucleon wave functions and taking the final state interaction into account by an approach which can be used when the value of the three-nucleon invariant mass is either below or above the pion emission threshold. Various kinematical conditions which enhance or minimize the effects of the final state interaction are thoroughly analyzed.

I. INTRODUCTION

The investigation of ground-state correlations (GSC) in nuclei, in particular those which originate from the most peculiar features of the nucleon-nucleon (NN) interaction, i.e., its strong short range repulsion and complex state dependence (spin, isospin, tensor, etc.), is one of the most challenging aspects of experimental and theoretical nuclear physics and, more generally, of hadronic physics. The results of sophisticated few- and many-body calculations in terms of realistic models of the NN interaction [1–3] show that the complex structure of the latter generates a rich correlation structure of the nuclear ground-state wave function. The experimental investigation of the nuclear wave function or, better, of various density matrices, $\rho(1), \rho(1,1'), \rho(1,2)$, etc., is therefore necessary in order to ascertain whether the prediction of the *standard model* of nuclei (structureless nonrelativistic nucleons interacting via the known NN forces) is indeed justified in practice, or other phenomena, e.g., relativistic effects, many-body forces, medium modification of nucleon properties, and explicit subnucleonic degrees of freedom (quark and gluons), have to be advocated in order to describe ground-state properties of nuclei at normal density and temperature.

Unfortunately, whereas the one-body density matrix (charge density) is experimentally well known since many years from elastic electron scattering (see, e.g., Ref. [4]), the present knowledge of those quantities which are more sensitive to GSC, e.g., the nondiagonal one-body and two-body density matrices, which could in principle be investigated by nucleon (N) emission processes like, e.g., the $A(e,e'N)X$ and $A(e,e'NN)X$ reactions, is still too scarce. The reason is that the effects from final state interactions (FSI), meson exchange currents (MEC), and isobar configuration (IC) creation may mask the effects generated by GSC. In our view, the present situation is such that the long-standing question whether FSI and other concurrent processes hinder the investigation of GSC, has not yet been clearly answered. Moreover, due to the difficulty to treat consistently GSC, FSI, MEC, etc., within the full complexity of the nuclear many-body approach, the answer was in the past merely dictated by

philosophical taste rather than by the results of solid calculations and unambiguous experimental data. A clear-cut answer to the above question would require, from one side, realistic many-body calculations of bound and continuum nuclear states, and, from the other side, a wise choice of the kinematics and of the type of process to be investigated, so as to possibly minimize all those effects which compete with GSC. In this respect, of particular usefulness is the two-proton emission process $A(e,e'pp)X$, where MEC play a minor role [with respect to the proton-neutron emission $A(e,e'pn)X$], since the virtual photon does not couple to the exchanged neutral meson, and IC production is also suppressed thanks to angular momentum and parity conservation selection rules (see, e.g., Ref. [5,6]).

The investigation of the two-nucleon emission processes has considerably progressed during the last few years, both in the few-body systems and the complex nuclei domains. In the latter case, extensive theoretical studies on the $A(e,e'pp)X$ process have been performed (see, e.g., Refs. [7–9] and references therein), aimed at developing various theoretical frameworks to treat GSC and FSI, together with competing effects, such as MEC, and, at the same time, experimental data have been obtained (see, e.g., Refs. [10,11]), which provided nontrivial evidence of GSC effects. The treatment of the two-nucleon emission process from few-body systems, which represents the object of the present investigation, has the nontrivial theoretical advantage that exact ground-state wave functions from variational or Faddeev-type calculations (see, e.g., Refs. [1,12,13] and references therein) can be used in the calculations, thus exploiting the whole realistic picture of GSC; moreover, provided the final three-nucleon invariant mass $\sqrt{s}$ is below the pion production threshold ($\sqrt{s} \simeq 2.95$ GeV), accurate continuum wave functions are also available [14], so that a fully consistent treatment of both GSC and FSI effects in the process $^3\text{He}(e,e'pp)n$ at low four-momentum transfer has been recently developed [1,14,30] Moreover, experimental data at low momentum transfer ($Q^2 \sim 0.1$ GeV/c^2, $Q^2 = \mathbf{q}^2 - \nu^2$, $\nu \sim 0.2$ GeV) became available from NIKHEF [15], which made it possible to produce a significant comparison between theoretical predictions and experimental data.

In this paper we are interested in medium and high momentum transfer regions; the reason is twofold: (i) by increasing the momentum transfer, one might be able to investigate the momentum space wave function in a broader

---

*On leave from Bogoliubov Lab. Theor. Phys., JINR, Dubna, Russia.

kinematical region; (ii) processes at high momentum transfer could provide crucial information on the origin and the very mechanism of hadronic rescattering in the medium [16], which has so far been investigated with simple three-body wave functions. Realistic calculations at intermediate and high values of Q^2 are therefore timely, also in view of running experiments at TJLab covering a region of intermediate values of Q^2 ($\nu \sim 0.4$–1 GeV, $Q^2 \sim 0.5$–2 GeV/c^2) [17]. It should be reminded, at this point, that when the momentum transfer is such that the three-nucleon invariant mass is higher than the pion production threshold, Faddeev-like calculations in the continuum cannot be performed, and the necessity arises for developing a proper treatment of elastic rescattering effects, in presence of inelastic channels. It is precisely the aim of this paper to present such a treatment, and to thoroughly analyze the possibility that by a proper choice of the kinematics, the effects of FSI in the process ^{3}He$(e,e'pp)n$ could be minimized. We would like to stress that our aim is not that of a direct comparison with (still lacking) experimental data in this region of momentum transfer, since, as previously stated, that would require a proper consideration of effects competing with GSC, but rather to try to understand whether particular kinematical conditions exist which could minimize the effects from FSI, a necessary condition for a meaningful investigation of GSC. Preliminary results of our calculations have already been presented in Ref. [18]. Through this paper we shall be using the three-body wave functions obtained by the Pisa group [13,19].

Our paper is organized as follows: in Sec. II some general concepts concerning the kinematics of the process and the cross section will be recalled; our approach to the treatment of FSI is illustrated in Sec. III, together with the results of calculations; the summary and conclusions are given in Sec. IV. Some useful formulas concerning two-nucleon correlations in nuclei are given in the Appendix.

II. KINEMATICS AND CROSS SECTION

We will consider the absorption of a virtual photon γ^* by a nucleon bound in ^{3}He, followed by two-nucleon emission, i.e., the process ^{3}He$(e,e'N_1N_2)N_3$, where N_1 and N_2 denote the nucleons which are detected. In the rest of this paper the photon four-momentum transfer will be denoted by

$$Q^2 = -q^2 = -(k_e - k_{e'})^2 = \mathbf{q}^2 - \nu^2 = 4\epsilon_e \epsilon_{e'} \sin^2 \frac{\theta_e}{2}, \quad (1)$$

where $k \equiv (\epsilon, \mathbf{k})$ is the four-momentum of the electron, $\mathbf{q} = \mathbf{k}_e - \mathbf{k}_{e'}$, $\nu = \epsilon_e - \epsilon_{e'}$, and $\theta_e \equiv \widehat{\theta_{\mathbf{k}_e \mathbf{k}_{e'}}}$.

The momenta of the bound nucleons, before γ^* absorption, will be denoted by $\mathbf{k}_i$, and after γ^* absorption, by $\mathbf{p}_i$. Momentum conservation requires that

$$\sum_{i=1}^{3} \mathbf{k}_i = 0, \quad \sum_{i=1}^{3} \mathbf{p}_i = \mathbf{q}, \quad (2)$$
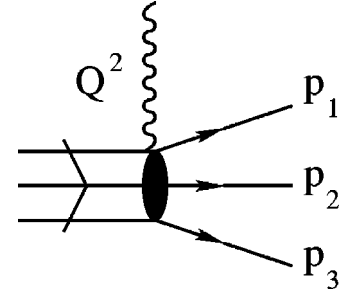
and energy conservation that

FIG. 1. The one photon exchange diagram for the two-nucleon (N) emission off ^{3}He, ^{3}He$(e,e'N_1N_2)N_3$. Q^2 is the four-momentum transfer and p_i denotes the four-momentum of nucleon N_i in the final state. N_1 and N_2 denote the detected nucleons.

$$\nu + M_3 = \sum_{i=1}^{3} (M_N^2 + \mathbf{p}_i^2)^{1/2}, \quad (3)$$

where M_N and M_3 are the masses of the nucleon and the three-nucleon system, respectively.

In one-photon exchange approximation, depicted in Fig. 1, the cross section of the process, reads as follows:

$$\frac{d^{12}\sigma}{d\epsilon_{e'} d\Omega_{e'} d\mathbf{p}_1 d\mathbf{p}_2 d\mathbf{p}_3}$$

$$= \sigma_{Mott} \cdot \sum_{\alpha=1}^{6} v_\alpha \cdot W_\alpha \cdot \delta\left(\mathbf{q} - \sum_{i=1}^{3} \mathbf{p}_i\right)$$

$$\times \delta\left(\nu + M_3 - \sum_{i=1}^{3} (M_N^2 + \mathbf{p}_i^2)^{1/2}\right), \quad (4)$$

where v_α are well known kinematical factors, and W_α the *response functions*, which have the following general form:

$$W_\alpha = |\langle \Psi_f^{(-)}(\mathbf{p}_1, \mathbf{p}_2, \mathbf{p}_3)|\hat{\mathcal{O}}_\alpha(\mathbf{q})|\Psi_i(\mathbf{k}_1, \mathbf{k}_2, \mathbf{k}_3)\rangle|^2. \quad (5)$$

In Eq. (5) $\Psi_f^{(-)}(\mathbf{p}_1, \mathbf{p}_2, \mathbf{p}_3)$ and $\Psi_i(\mathbf{k}_1, \mathbf{k}_2, \mathbf{k}_3)$ are the continuum and ground-state wave functions of the three-body system, respectively, and $\hat{\mathcal{O}}_\alpha(\mathbf{q})$ is a quantity depending on proper combinations of the components of the nucleon current operator $\hat{j}^\mu$ (see, e.g., Ref. [4]). Two nucleon emission originated by NN correlations can occur because of two different processes:

(i) In the initial state "1" and "2" are correlated and "3" is far apart; γ^* is absorbed either by 1 or 2 and all of the three-nucleons are emitted in the continuum; if nucleon 3 was at rest in the initial state, one has $\mathbf{k}_1 = -\mathbf{k}_2$ and, if FSI is disregarded, $\mathbf{p}_{1(2)} = \mathbf{k}_{1(2)} + \mathbf{q}$, $\mathbf{p}_{2(1)} = \mathbf{k}_{2(1)}$ in the final state.

(ii) In the initial state nucleons 1 and 2 are correlated and 3 is far apart; γ^* is absorbed by N_3 and all of the three-nucleons are emitted in the continuum. If N_3 was at rest before interaction, and FSI is disregarded, N_1 and N_2 are emitted back-to-back with momenta $\mathbf{k}_1 = -\mathbf{k}_2$ and $\mathbf{p}_3 = \mathbf{q}$.

The above picture is distorted by FSI. The aim of this paper is precisely to investigate the relevance of FSI effects in both processes.
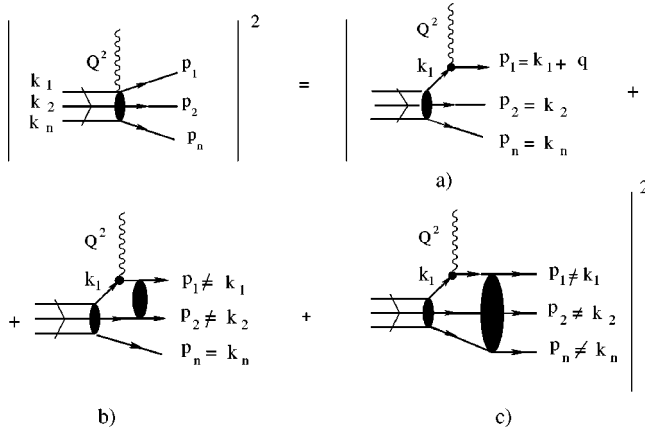
FIG. 2. Schematic representation of the various processes contributing to the reaction $^3\text{He}(e,e'p_1 p_2)n$: (a) denotes the plane wave approximation (PWA), (b) the pp rescattering, (c) the three-body rescattering. $k_1(p_1), k_2(p_2)$, and $k_n(p_n)$ denote the momenta of proton 1, proton 2, and the neutron, respectively, in the initial (final) state.

III. FINAL STATE INTERACTION IN THE TWO-NUCLEON EMISSION PROCESS

We will now assume that N_1 and N_2, the two detected nucleons, are the two protons and N_3 the neutron (n). The two-nucleon emission process will thus be $^3\text{H}(e,e'p_1 p_2)n$ which, as explained, can originate from the two mechanisms described above.

A. Process 1: Absorption of γ^* by the correlated pp pair

In this process γ^* is absorbed by proton 1 (2) correlated with proton 2 (1), and the neutron is the "spectator."

The various diagrams, in order of increasing complexity, which contribute to the process are depicted in Fig. 2.

Let us introduce the following quantities:

(i) the *relative momentum* of the detected proton pair

$$\mathbf{p}_{rel} = \frac{\mathbf{p}_1 - \mathbf{p}_2}{2} \equiv \mathbf{t}; \qquad (6)$$

(ii) the *center-of-mass momentum* of the pair

$$\mathbf{P} = \mathbf{p}_1 + \mathbf{p}_2. \qquad (7)$$

In what follows, for ease of presentation, and also in order to make the comparison with previous calculations more transparent, we will consider the effects of the FSI on the longitudinal response only. Let us first consider Figs. 2(a) and (b), i.e., the plane wave approximation plus the pp rescattering in the final state. By changing the momentum variables from $\mathbf{p}_1$ and $\mathbf{p}_2$ to $\mathbf{P}$ and $\mathbf{p}_{rel}$, and integrating the cross section [Eq. (4)] over $\mathbf{P}$ and the kinetic energy of the neutron, we obtain

$$\frac{d^8\sigma}{d\epsilon_{e'} d\Omega_{e'} d\Omega_{p_n} dp_{rel} d\Omega_{p_{rel}}}$$
$$= \mathcal{K}(Q^2, \nu, \mathbf{p}_n, \mathbf{p}_{rel}) \cdot R_L(\nu, Q^2, \mathbf{p}_n, \mathbf{p}_{rel}) \qquad (8)$$

with

$$R_L(\nu, Q^2, \mathbf{p}_n, \mathbf{p}_{rel}) = G_E^p(Q^2)^2 \cdot M^{(pp)}(\mathbf{p}_n, \mathbf{p}_{rel}, \mathbf{q}), \qquad (9)$$

where $G_E^p(Q^2)$ is the proton electric form factor, $\mathcal{K}$ incorporates all kinematical variables, and $M^{(pp)}(\mathbf{p}_n, \mathbf{p}_{rel}, \mathbf{q})$ is the transition nuclear form factor which includes the pp rescattering, viz.,

$$M^{(pp)}(\mathbf{p}_n, \mathbf{p}_{rel}, \mathbf{q})$$
$$= \frac{1}{2} \sum_{\mathcal{M}} \sum_{S_{pp}, \Sigma_{pp}} \sum_{\sigma_n} |T^{(pp)}(\mathcal{M}, \sigma_n, S_{pp}, \Sigma_{pp}, \mathbf{p}_n, \mathbf{p}_{rel}, \mathbf{q})|^2. \qquad (10)$$

The scattering matrix $T^{(pp)}(\mathcal{M}, \sigma_n, S_{pp}, \Sigma_{pp}, \mathbf{p}_n, \mathbf{p}_{rel}, \mathbf{q})$ has the following form:

$$T^{(pp)}(\mathcal{M}, \sigma_n, S_{pp}, \Sigma_{pp}, \mathbf{p}_n, \mathbf{p}_{rel}, \mathbf{q})$$
$$= \int d^3r d^3\rho \, \Psi_{(1/2)\mathcal{M}}(\mathbf{r}, \boldsymbol{\rho}) \chi_{(1/2)\sigma_n}$$
$$\times \exp(-i\mathbf{p}_n\boldsymbol{\rho}) \psi_{S_{pp}, \Sigma_{pp}}^{\text{t}(-)}(\mathbf{r}) \exp(i\mathbf{q}\mathbf{r}/2), \qquad (11)$$

where $\Psi_{(1/2)\mathcal{M}}(\mathbf{r}, \boldsymbol{\rho})$ is the three-nucleon wave function, $\psi_{S_{pp}, \Sigma_{pp}}^{\text{t}}(\mathbf{r})$ the continuum two-proton wave function, and $\chi_{(1/2)\sigma_n}$ the neutron spinor. In the above and the following equations, $\mathbf{r}$ and $\boldsymbol{\rho}$ are the Jacobi coordinates:

$$\mathbf{r} = \mathbf{r}_1 - \mathbf{r}_2, \qquad \boldsymbol{\rho} = \mathbf{r}_3 - \frac{1}{2}(\mathbf{r}_1 + \mathbf{r}_2). \qquad (12)$$

When pp rescattering is disregarded, i.e., only Fig. 2(a) is considered, one has

$$\mathbf{p}_1 = \mathbf{k}_1 + \mathbf{q}, \qquad \mathbf{p}_2 = \mathbf{k}_2, \qquad \mathbf{p}_n = \mathbf{k}_n, \qquad (13)$$

$$\mathbf{p}_{rel} = \mathbf{k}_{rel} + \frac{\mathbf{q}}{2}, \qquad \mathbf{P} = \mathbf{K} + \mathbf{q}, \qquad (14)$$

where

$$\mathbf{k}_{rel} = \frac{\mathbf{k}_1 - \mathbf{k}_2}{2}, \qquad \mathbf{K} = \mathbf{k}_1 + \mathbf{k}_2 = -\mathbf{k}_n \qquad (15)$$

are the relative and center of mass (c.m.) momenta of the pp pair before interaction. The two-proton continuum wave function is simply $\psi_{S_{pp}, \Sigma_{pp}}^{\text{t}}(\mathbf{r}) = \chi_{S_{pp}, \Sigma_{pp}} \exp(i\mathbf{p}_{rel}\mathbf{r})$ and the scattering amplitude becomes

$$T^{(pp)}(\mathcal{M}, \sigma_n, S_{pp}, \Sigma_{pp}, \mathbf{p}_n, \mathbf{p}_{rel}, \mathbf{q})$$
$$\rightarrow T^{(PWA)}(\mathcal{M}, \sigma_n, S_{pp}, \Sigma_{pp}, \mathbf{k}_n, \mathbf{k}_{rel})$$
$$= \int d^3r d^3\rho \, \Psi_{(1/2)\mathcal{M}}(\mathbf{r}, \boldsymbol{\rho}) \chi_{(1/2)\sigma_n}$$
$$\times \exp(-i\mathbf{k}_n\boldsymbol{\rho}) \chi_{S_{pp}, \Sigma_{pp}} \exp(-i\mathbf{k}_{rel}\mathbf{r}), \qquad (16)$$

which is nothing but the three-body wave function in momentum space.

The scattering amplitude which includes the pp rescattering has been calculated using the continuum wave function for two interacting protons:

$$\psi_{S_{pp},\Sigma_{pp}}^{\mathbf{t}}(\mathbf{r})=4\pi\sum_{lm}\sum_{l'S'J_f}\langle lmS_{pp}\Sigma_{pp}|J_fM_J\rangle i^{l'}Y_{lm}^*$$

$$\times(\hat{\mathbf{p}}_{rel})R_{lSl'S'}^{J_f}(r)Y_{l'S'}^{J_fM_J}(\hat{\mathbf{r}}), \qquad (17)$$

where $Y_{lm}(\hat{\mathbf{p}}_{rel})[Y_{l'S'}^{J_fM_J}(\hat{\mathbf{r}})]$ denotes the spherical (spin-angular) harmonics, and $R_{lSl'S'}^{J_f}(r)$ is the scattering radial wave function, solution of the Schrödinger equation in the continuum, with asymptotic behavior,

$$R_{lSl'S'}^{J_f}(r)|_{r\to\infty}\to\delta_{ll'}\delta_{SS'}\exp(i\delta_l)\frac{\sin[tr-(l\pi/2)+\delta_l]}{tr}, \qquad (18)$$

where $t\equiv|\mathbf{t}|\equiv|\mathbf{p}_{rel}|$. In the presence of a tensor interaction the asymptotic of $R_{lSl'S'}^{J_f}(r)$ is more complicated but, by a unitary transformation, other radial wave functions may be introduced with asymptotic similar to Eq. (18) (see, e.g., Ref. [20]).

Inserting Eq. (17) into Eq. (11), and using the completeness of the scattering wave functions, the amplitude T^{pp} in Eq. (10) can be expressed in the following way:

$$T^{(pp)}(\mathcal{M},\sigma_n,S_{pp},\Sigma_{pp},\mathbf{p}_n,\mathbf{p}_{rel},\mathbf{q})$$

$$=\frac{2}{\pi}\int \tilde{t}^2 d\tilde{t} d^3\rho d^3r \exp(-i\mathbf{p}_n\boldsymbol{\rho})$$

$$\times\sum_{\{\alpha\}}\langle XM_XL_\rho M_\rho|\tfrac{1}{2}\mathcal{M}\rangle\langle j_{12}M_{12}\tfrac{1}{2}\sigma_3|XM_X\rangle$$

$$\times\langle l_{12}m_{12}S_{pp}\nu|j_{12}M_{12}\rangle\langle l_fm_fS_{pp}\Sigma_{pp}|j_fM_f\rangle$$

$$\times\langle l_f\tilde{m}_fS_{pp}\nu|j_fM_f\rangle Y_{l_fm_f}(\hat{\mathbf{p}}_{rel})Y_{l_{12}m_{12}}(\hat{\mathbf{r}})Y_{l_f\tilde{m}_f}^*(\hat{\mathbf{r}})$$

$$\times\exp(i\mathbf{q}\mathbf{r}/2)R_{l_{12}S_{pp}}^{j_{12},\tilde{t}}(r)R_{l_fS_{pp}}^{j_f,t}(r)(-i)^{l_f}I_{\{\alpha\}}^{|\tilde{\mathbf{p}}_{rel}|}(|\boldsymbol{\rho}|), \qquad (19)$$

where $\{\alpha\}$ denotes the full set of quantum numbers characterizing the ground-state partial configurations in the ^{3}He wave function, and $I_{\{\alpha\}}^{|\tilde{\mathbf{p}}_{rel}|}(|\boldsymbol{\rho}|)$ are the corresponding overlaps with the scattering state wave functions.

In what follows the so-called *symmetric* (sym) kinematics [21]

$$\mathbf{p}_n=0;\quad \mathbf{p}_1+\mathbf{p}_2=\mathbf{q}$$

will be considered, which corresponds, in plane wave approximation (PWA), to a ground-state configuration characterized by the two protons with equal and opposite momenta and the neutron with zero momentum. In the sym kinematics, the transition form factor $M^{(pp)}(\mathbf{p}_n,\mathbf{p}_{rel},\mathbf{q})$, when γ^* inter-

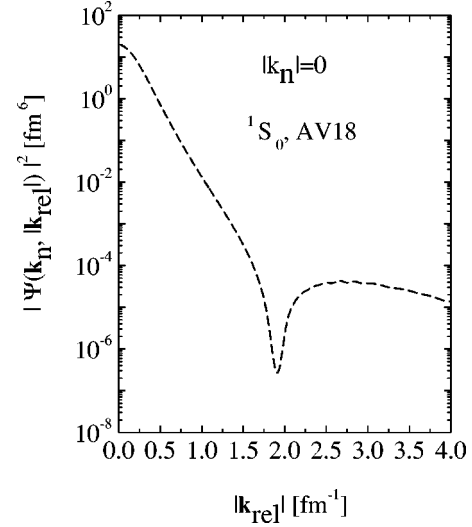FIG. 3. The momentum space wave function of ^{3}He corresponding to the configuration in which the neutron is at rest and the two protons are in the state $^1S_0$ of relative motion with momentum $\mathbf{k}_{rel}=(\mathbf{k}_1-\mathbf{k}_2)/2$. Three-body wave function from Ref. [19]; AV18 interaction [22].

acts with proton 1(2), will only depend upon $\mathbf{p}_{rel}=\mathbf{q}/2 -\mathbf{p}_{2(1)}$, i.e., for a fixed value of $|\mathbf{q}|$, will only depend upon $|\mathbf{p}_{2(1)}|$ and the angle between $\mathbf{q}$ and $\mathbf{p}_{2(1)}$. In PWA, when the angular momentum of the neutron is zero, also the pp pair has relative angular momentum zero, so that the cross section is almost entirely determined by the square of the $^1S_0$ component of the three-body wave function $\Psi(\mathbf{k}_{rel},\mathbf{k}_n =0)$, which is shown in Fig. 3.

The calculated transition form factor is shown in Fig. 4. Calculations have been performed with three-body wave function obtained in Ref. [19] using the Argonne v-18 (AV18) interaction [22]. Our results, which are in agreement with the ones of Ref. [21] (where a different ground-state wave function has been used), show that the pp rescattering is very large and completely distorts the PWA results.

In order to investigate to what extent FSI depend upon the kinematics of the process, we have also considered the *superparallel* (sp) kinematics, according to which one still has $\mathbf{p}_n=0$, $\mathbf{p}_1+\mathbf{p}_2=\mathbf{q}$, but all momenta are collinear, i.e., $(\mathbf{q}\|z)$,

$$\mathbf{p}_{1\perp}=\mathbf{p}_{2\perp}=0,\quad p_{1z}+p_{2z}=|\mathbf{q}|. \qquad (20)$$

The results of calculations, which are presented in Fig. 5, look very different from the ones shown in Fig. 4. Concerning these differences, the following remarks are in order:

(i) As far as the PWA results are concerned, it can be seen that the transition matrix elements differ, at the same value of ν, by more than one order of magnitude; the reason is that the relative momentum $|\mathbf{k}_{rel}|$, at a given value of ν, is very different in the two kinematics, with $|\mathbf{k}_{rel}^{(sym)}|\gg|\mathbf{k}_{rel}^{(sp)}|$ (e.g., at $\nu=0.2$ GeV one has $|\mathbf{k}_{rel}^{(sp)}|\simeq0.45$ fm^{-1}, whereas $|\mathbf{k}_{rel}^{(sym)}| \simeq2.2$ fm^{-1}). Since in both kinematics $M^{PWA}(\mathbf{k}_n,\mathbf{k}_{rel})$ is entirely determined by the $^1S_0$ three-body wave function $\Psi(|\mathbf{k}_{rel}|,\mathbf{k}_n=0)$, the value of ν at which this exhibits its minimum is different in the two cases.
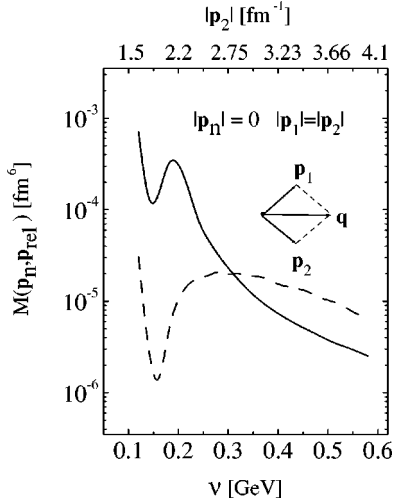
FIG. 4. The transition form factor $M(\mathbf{p_n},\mathbf{p_{rel}},\mathbf{q})$ [Eq. (10)] calculated in the symmetric kinematics [21]: $\mathbf{p}_1+\mathbf{p}_2=\mathbf{q}$, $\mathbf{p}_n=0$, $|\mathbf{p}_1|=|\mathbf{p}_2|=\sqrt{\frac{1}{4}(\nu+M_3-M_n)^2-M_p^2}$, $\mathbf{p}_{rel}=\mathbf{q}/2-\mathbf{p}_2$, $\theta_{12}=2\arccos|\mathbf{q}|/2|\mathbf{p}_2|$. The dashed line corresponds to the plane wave approximation (PWA) [plane waves for the three-nucleons, process (a) in Fig. 2], whereas the full line includes the pp rescattering [process (a) + process (b) in Fig. 2]. The value of $|\mathbf{q}|$ corresponds to $\epsilon_e=2$ GeV and $\theta_e=15°$ [cf. Eq. (1)], and the range of its variation with ν is $0.52 \leq |\mathbf{q}| \leq 0.75$ GeV/c. Three-body wave function from Ref. [19]; AV18 interaction [22].

(ii) In Fig. 4 the pp rescattering effects depend upon the value of the relative momentum of the two protons in the final state $|\mathbf{p}_{rel}|=|\mathbf{p}_1|\sin(\theta_{12}/2)\neq|\mathbf{k}_{rel}|$. Unlike the PWA case, one has $|\mathbf{p}_{rel}^{(sym)}| \lesssim |\mathbf{p}_{rel}^{(sp)}|$ [e.g., at $\nu=0.2$ GeV one has $|\mathbf{q}|\simeq535$ MeV/c, $|\mathbf{p}_2|\simeq0.45$ fm^{-1}, and $|\mathbf{p}_{rel}|\simeq1.8$ fm^{-1}, in the sp kinematics, and $|\mathbf{p}_1|=|\mathbf{p}_2|\simeq2.2$ fm^{-1}, $\theta_{12}\simeq105°$, and $|\mathbf{p}_{rel}|=|\mathbf{p}_1|\sin(\theta_{12}/2)\simeq1.7$ fm^{-1} in the sym kinematics]. Thus the two-proton relative energy in the final state is larger in the sp kinematics, which explains the appar-
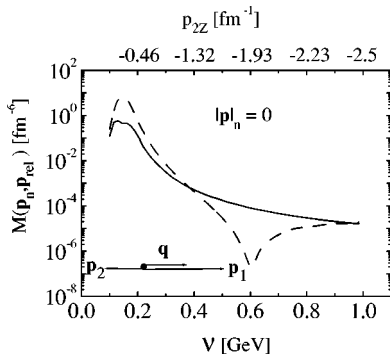

FIG. 5. The transition form factor $M(\mathbf{p_n},\mathbf{p_{rel}},\mathbf{q})$ [Eq. (10)] calculated in the superparallel kinematics ($\mathbf{p}_{1\perp}=\mathbf{p}_{2\perp}=0$, $p_{1z}+p_{2z}=|\mathbf{q}|$, with $\mathbf{q}\|z$). The dashed line corresponds to the plane wave approximation (PWA) [plane waves for the three-nucleons, process (a) in Fig. 2], whereas the full line includes the pp rescattering [process (a) + process (b) in Fig. 2]. The value of $|\mathbf{q}|$ corresponds to $\epsilon_e=2$ GeV and $\theta_e=15°$ [cf. Eq. (1)] and the range of its variation with ν is $0.52 \leq |\mathbf{q}| \leq 1.0$ GeV/c. Three-body wave function from Ref. [19]; AV18 interaction [22].

ent smaller effects of FSI in Fig. 5. In this respect, it should, however, be pointed out that at values of $\nu>0.7-0.8$ GeV, i.e., at large values of $p_{2z}\gtrsim1$ fm^{-1}, where correlation effects are more relevant, the momentum transfer $|\mathbf{q}|$ and the relative momentum of the proton pair become very large, and the Schrödinger equation cannot in principle be applied to describe the pp interaction in the continuum (e.g., in the sp kinematics, when $|\mathbf{q}|\gtrsim1$ GeV/c, $|\mathbf{p}_2|\simeq0.5$ GeV/c, $|\mathbf{p}_1|\simeq1.5$ GeV/c, $|\mathbf{p}_{rel}|\simeq1$ GeV/c). To treat the case of high energies, a Glauber-type calculation is in progress and will be reported elsewhere [24]. Thus it appears that in the sp kinematics considered in Fig. 5, there exists only a small bin of $\nu\simeq0.4-0.5$ GeV where two-nucleon correlations could be investigated treating the pp rescattering within the Schrödinger equation.

The next contribution to be considered is the proton-neutron rescattering [Fig. 2(c)]. This has been found in Ref. [21] to provide very small effects, as also recently found in Ref. [18]. This point will be discussed in detail in the next section.

B. Process 2: Absorption of γ^* by the neutron

1. Plane wave approximation and the pp rescattering

We will now consider the process ^{3}He$(e,e'p_1p_2)n$, in which γ^* interacts with the neutron and the two protons are emitted and detected. We will consider two extreme cases of this process, viz., (i) in the initial state the neutron is a partner of a correlated proton-neutron pair, with the second proton far apart from the pair; (ii) in the initial state the neutron is at rest, far apart from the two correlated protons. Process (ii) has been considered in Ref. [14] for the case of both a neutron and a proton at rest in the initial state. We will compare our results with the ones of Ref. [14], considering only the case of the neutron at rest. The various mechanisms, in order of increasing complexity, which contribute to the above process, are depicted in Fig. 6.

When the final state rescattering between the two protons is taken into account [the process of Fig. 6(a) plus the process of Fig. 6(b)], but the interaction of the hit neutron with the emitted proton-proton pair is disregarded, one has $\mathbf{p}_n=\mathbf{k}_n+\mathbf{q}$, and the cross section [Eq. (4)] integrated over $\mathbf{P}$ and the kinetic energy of the neutron exhibits the same structure of Eq. (8), with R_L given by

$$R_L(\nu,Q^2,\mathbf{p}_n,\mathbf{p}_{rel})=G_E^n(Q^2)^2\cdot M^{(pp)}(\mathbf{p}_n,\mathbf{p}_{rel},\mathbf{q}) \quad (21)$$

which differs from Eq. (9) in two respects: (i) the proton electric form factor is replaced by the neutron one $G_E^n(Q^2)$; (ii) $M^{(pp)}(\mathbf{p}_n,\mathbf{p}_{rel},\mathbf{q})$ includes the rescattering *between the two spectator protons* and not between the active and recoiling protons; this means that T^{pp} has the following form:

$$T^{pp}(\mathcal{M},\sigma_n,S_{pp},\Sigma_{pp},\mathbf{k}_n,\mathbf{p}_{rel})$$

$$=\int d^3\rho\exp(-i\mathbf{k}_n\boldsymbol{\rho})\chi_{(1/2)\sigma_n}I_{\mathcal{M},S_{pp},\Sigma_{pp}}^{t,pp}(\boldsymbol{\rho}), \quad (22)$$

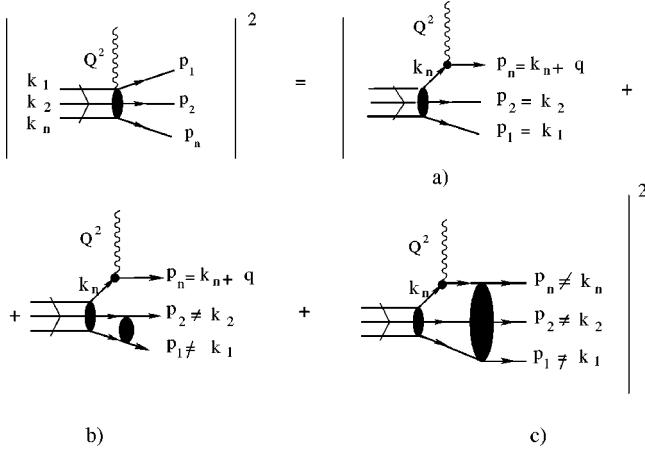FIG. 6. Schematic representation of the various processes contributing to the reaction ^{3}He$(e,e'p_1p_2)n$ when γ^* is absorbed by the neutron, and the two protons are emitted in the continuum: (a) denotes the plane wave approximation (PWA), (b) the pp rescattering, (c) the three-body rescattering. The sum of contributions (a) and (b) is referred to by some authors as the *plane wave impulse approximation* (PWIA); in Ref. [14] PWIA is used, on the contrary, to denote our (symmetrized) PWA approximation. In the rest of this paper we shall be using the term PWA to denote process (a), and the term *pp rescattering* to denote process (b). Note, moreover, that in Ref. [14] our pp rescattering contribution is called "tG_0."

where $\mathbf{k}_n = \mathbf{p}_n - \mathbf{q} = -(\mathbf{p}_1 + \mathbf{p}_2)$, and I^t is the *overlap integral* between the three-nucleon ground-state wave function and the two-proton continuum state, i.e.,

$$I^{t,pp}_{\mathcal{M},S_{pp},\Sigma_{pp}}(\boldsymbol{\rho}) = \int \psi^{t(-)}_{S_{pp},\Sigma_{pp}}(\mathbf{r})\Psi_{(1/2)\mathcal{M}}(\mathbf{r},\boldsymbol{\rho})d^3r. \quad (23)$$

We reiterate that in the process analyzed in the previous section, the pp rescattering occurred between the protons of the *active pair* which absorbed the virtual photon, whereas in this case γ^* is absorbed by the neutron and the pp rescattering involves the two *spectator* protons. Within the PWA, i.e., when only process of Fig. 6(a) contributes to the reaction, one has $\psi^t_{S_{pp},\Sigma_{pp}}(\mathbf{r}) = \chi_{S_{pp},\Sigma_{pp}}\exp(i t\mathbf{r})$ so that

$$I^{t,PWA}_{N_2N_3}(\boldsymbol{\rho}) = \int \Psi_{(1/2)\mathcal{M}}(\mathbf{r},\boldsymbol{\rho})\chi_{S_{pp},\Sigma_{pp}}\exp(-i t\mathbf{r})d^3r \quad (24)$$

and

$$T^{PWA}(\mathcal{M},\sigma_n,S_{pp},\Sigma_{pp},\mathbf{k}_n,\mathbf{k}_{rel})$$
$$= \int d^3r d^3\rho \Psi_{(1/2)\mathcal{M}}(\mathbf{r},\boldsymbol{\rho})\chi_{(1/2)\sigma_n}$$
$$\times \exp(-i\mathbf{k}_n\boldsymbol{\rho})\chi_{S_{pp},\Sigma_{pp}}\exp(-i\mathbf{k}_{rel}\mathbf{r}), \quad (25)$$

which, as in process 1, is nothing but the three-nucleon wave function in momentum space.

It is interesting to point out that the integral of the transition form factor (22) over the direction of $\mathbf{p}_{rel}$ is related to the neutron spectral function $P_1(k_n,E^*)$ [23],

$$P_1(k_n,E^*) = \frac{|\mathbf{p}_{rel}|M_N}{(2\pi)^4}\sum_{\mathcal{M},S_{pp},\Sigma_{pp},\sigma_n}\int d\Omega_t \left| \int d^3r d^3\rho \right.$$
$$\times \exp(-i\mathbf{k}_n\boldsymbol{\rho})\chi_{(1/2)\sigma_n}\psi^{t(-)}_{S_{pp}\Sigma_{pp}}(\mathbf{r})$$
$$\times \left. \Psi_{(1/2)\mathcal{M}}(\mathbf{r},\boldsymbol{\rho}) \right|^2, \quad (26)$$

by the following relation:

$$\int \mathcal{P}_1(\mathbf{k}_n,\mathbf{p}_{rel})d\Omega_{\mathbf{p}_{rel}} = P_1(k_n,E^*), \quad (27)$$

where

$$\mathcal{P}_1(\mathbf{k}_n,\mathbf{p}_{rel}) = \frac{M_N|\mathbf{p}_{rel}|}{2}M^{pp}(\mathbf{k}_n,\mathbf{p}_{rel}) \quad (28)$$

will be called here the vector spectral function, and

$$E^* = \frac{\mathbf{p}_{rel}^2}{M} = \frac{(\mathbf{p}_1-\mathbf{p}_2)^2}{4M} \quad (29)$$

is the "excitation energy" of the spectator pp pair, which is related to the *neutron removal energy E* by the relation $E = E_3 + E^*$, where E_3 is the (positive) binding energy of the three-nucleon system (cf. Ref. [23]).

The cross section for the two-proton emission process can then be written in the following form:

$$\frac{d^8\sigma}{d\epsilon_{e'}d\Omega_{e'}d\Omega_{p_n}dp_{rel}d\Omega_{p_{rel}}}$$
$$= \mathcal{K}(Q^2,\nu,\mathbf{p}_n,\mathbf{p}_{rel})\cdot 2\frac{G^n_E(Q^2)}{M_N|\mathbf{p}_{rel}|}\mathcal{P}_1(\mathbf{k}_n,\mathbf{p}_{rel}). \quad (30)$$

By integrating over $\Omega_{p_{rel}}$, one obtains the cross section for the semi-inclusive process ^{3}He$(e,e'n)pp$,

$$\frac{d^6\sigma}{d\epsilon_{e'}d\Omega_{e'}d\Omega_n dp_{rel}} = \mathcal{K}G^n_E(Q^2)^2\cdot P_1(k_n,E^*). \quad (31)$$

The neutron spectral function calculated with and without the pp rescattering [23] is shown in Fig. 7. It can be seen that at $k_n \gtrsim 1.5$ fm^{-1} there are regions, peaked at $E^* \simeq \mathbf{k}_n^2/4M$, where the pp rescattering does not play any role; since $E^* = \mathbf{p}_{rel}^2/M$, at the peaks we have the following relation between $|\mathbf{k}_n|$ and $|\mathbf{p}_{rel}|$:

$$|\mathbf{k}_n| \simeq 2|\mathbf{p}_{rel}|. \quad (32)$$

The positions of the peaks have been originally interpreted as arising from a *two-nucleon correlation* (2NC) configuration, where proton 1 (2) is correlated with the neutron with momenta satisfying the following relations: $\mathbf{k}_{2(1)} = 0$, $\mathbf{k}_{1(2)} \simeq -\mathbf{k}_n$ [26]; moreover, the energy dependence around the peaks can be related to the motion of the third particle
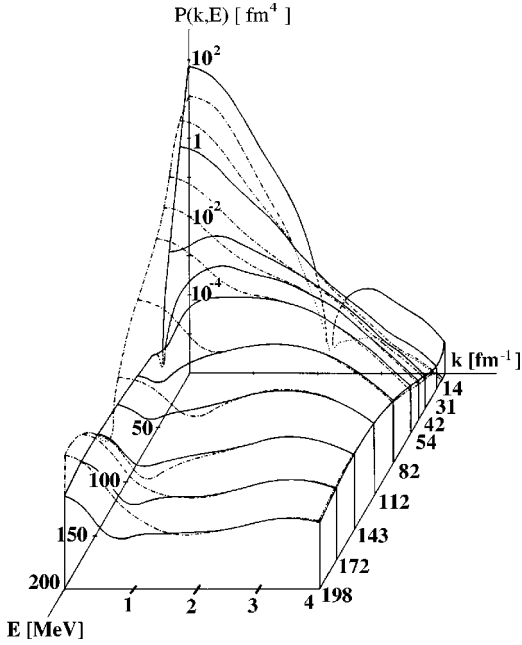
FIG. 7. The neutron spectral function in ^{3}He ($k \equiv |\mathbf{k}_n|$) corresponding to the three-body channel ^{3}He$\rightarrow (pp) - n$. The dot-dashed line represents the PWA, whereas the full line includes the proton-proton rescattering. Three-nucleon wave function from Ref. [23]; Reid soft core interaction [25] adapted from. Ref. [23].

$\mathbf{k}_{2(1)} \neq 0$, or, equivalently, to the center-of-mass motion of the correlated pair [27]. The existence of the region where pp rescattering is vanishing is a general feature of any spectral function, independent of the two-nucleon interaction and of the method to generate the wave function. This is illustrated in Fig. 8, where the spectral function corresponding to the variational three-body wave function of Ref. [19] ob-
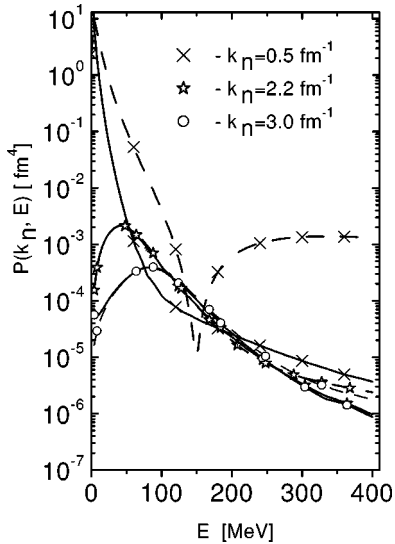

FIG. 8. The same as in Fig. 7 but with the three-body wave function from Ref. [19] and the AV18 interaction [22]. The E dependence of the spectral function is shown for three values of the neutron momentum. The dashed line represents the PWA results, whereas the full line includes the pp rescattering.
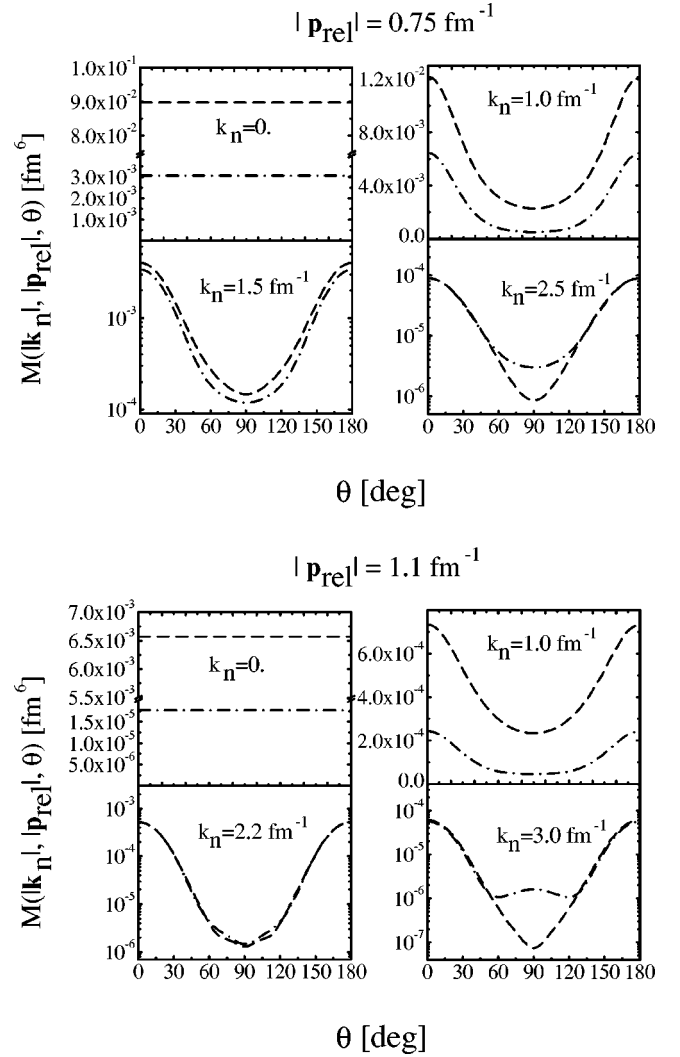

FIG. 9. Top panel. Dashed line: the transition form factor $M^{pp}(\mathbf{k}_n, \mathbf{p}_{rel}) \equiv (2/M_N|\mathbf{p}_{rel}|)\mathcal{P}_1(\mathbf{k}_n, \mathbf{p}_{rel})$ [see Eq. (28)] plotted *vs* the angle θ between $\mathbf{k}_n$ and $\mathbf{p}_{rel}$ for various values of $k_n \equiv |\mathbf{k}_n|$ and $|\mathbf{p}_{rel}| = 0.75$ fm^{-1} (the corresponding "excitation energy" of the pp pair is $E^* = |\mathbf{p}_{rel}|^2/M_N \simeq 23$ MeV). Dot-dashed line: the same quantity in the PWA, i.e., disregarding the pp rescattering. Three-body wave function from Ref. [19]; AV18 interaction [22]. Bottom panel: The same as in the top panel for $|\mathbf{p}_{rel}| = 1.1$ fm^{-1} ($E^* = |\mathbf{p}_{rel}|^2/M_N \simeq 50$ MeV).

tained with the AV18 interaction [22], is shown for several values of $k \equiv |\mathbf{k}_n|$. It can be seen that for values of k_n which satisfy relation (32), FSI effects generated by pp rescattering are negligible.

Relation (32) does not necessarily imply a 2NC configuration, i.e., $\mathbf{k}_{2(1)} = 0$, $\mathbf{k}_{1(2)} \simeq -\mathbf{k}_n$, for it holds also if $\mathbf{k}_{2(1)} \neq 0$, $\mathbf{k}_{1(2)} \neq -\mathbf{k}_n$. The analysis of the vector spectral function $\mathcal{P}_1(|\mathbf{k}_n|, |\mathbf{p}_{rel}|, \theta)$ should tell us what are the dominant configurations in the three-body wave function. To this end, we have plotted the vector spectral function *vs* θ in correspondence of two values of $|\mathbf{p}_{rel}|$: $|\mathbf{p}_{rel}| = 0.75$ fm^{-1} ($E^* = |\mathbf{p}_{rel}|^2/M \simeq 23$ MeV) and $|\mathbf{p}_{rel}| = 1.1$ fm^{-1} ($E^* = |\mathbf{p}_{rel}|^2/M \simeq 50$ MeV) and various values of k_n. The

re-sults, which are shown in Fig. 9, deserve the following comments:

(i) The constant behavior of $\mathcal{P}_1$ at $k_n = 0$ can easily be understood by considering that, as previously discussed, only the angle independent $^1S_0$ pp wave function contributes.

(ii) Equation (32), i.e., the relation $|\mathbf{k}_n| = 2|\mathbf{p}_{rel}|$, would correspond to $|\mathbf{k}_n| \simeq 1.5$ fm^{-1}, when $|\mathbf{p}_{rel}| = 0.75$ fm^{-1}, and to $|\mathbf{k}_n| \simeq 2.2$ fm^{-1}, when $|\mathbf{p}_{rel}| = 1.1$ fm^{-1}. It can be seen that when $|\mathbf{k}_n| = 2|\mathbf{p}_{rel}|$ pp rescattering effects almost disappear, but they become extremely large when such a relation is not satisfied, except when $|\mathbf{k}_n| \gtrsim 2|\mathbf{p}_{rel}|$ *and* $\theta \simeq 0°, 180°$.

(iii) When $|\mathbf{k}_n| = 2|\mathbf{p}_{rel}|$, the value $\theta = 0° (180°)$ (super-parallel kinematics), corresponds to $|\mathbf{k}_{1(2)}| = 0$, $\mathbf{k}_n = -\mathbf{k}_{2(1)}$, i.e., to the 2NC configuration (see the Appendix). The results presented in Fig. 9 clearly show that such a configuration is the dominant one; as a matter of fact, far from such a configuration (e.g., at $\theta = 90°$, when three-nucleon configurations are important), the vector spectral function is sensibly smaller. Thus the most probable configuration in the three-nucleon wave function, when $|\mathbf{k}_n| = 2|\mathbf{p}_{rel}|$, is indeed the 2NC configuration, when one nucleon of the pp pair is almost at rest and the second one has momentum almost equal and opposite to the momentum of the neutron.

(iv) When $|\mathbf{k}_n| \neq 2|\mathbf{p}_{rel}|$ and $\theta \simeq 0°, 180°$, we still stay in the superparallel kinematics but not in the two-nucleon correlation region, for now $|\mathbf{k}_{2(1)}| \neq 0$, $\mathbf{k}_n \neq -\mathbf{k}_{1(2)}$; however, it can be seen that for $|\mathbf{k}_n| > 2|\mathbf{p}_{rel}|$, when the violation of the condition $|\mathbf{k}_n| = 2|\mathbf{p}_{rel}|$ is very mild, pp rescattering effects are still very small; note, moreover, that if the FSI can only be described by the pp rescattering, the cross section should be the same at both angles, a behavior which deserves experimental investigation.

Thus the study of the vector spectral function at $|\mathbf{k}_n| \simeq 2|\mathbf{p}_{rel}|$, $\theta \simeq 0°$ or $180°$, which could be undertaken by measuring the $(e, e'2p)$ process in the superparallel kinematics, would allow one to obtain information on the three-nucleon wave function in momentum space, provided the rescattering of the two protons with the outgoing neutron does not appreciably distort the process. The full calculation of the transition matrix element at low momentum transfer has been undertaken in Ref. [14] within a consistent Faddeev approach to bound and continuum states of the three-nucleon system. The process considered in Ref. [14] is the absorption of γ^* by a neutron (proton) at rest with the two protons (proton-neutron) emitted back to back with equal momenta $\mathbf{p}_1 = -\mathbf{p}_2 \equiv \mathbf{p}$ and the neutron with momentum $\mathbf{p}_n = \mathbf{q}$ emitted in a direction perpendicular to $\mathbf{p}$. Thanks to the fully consistent treatment of bound and continuum state wave functions, the calculation presented in Ref. [14] represents the state of the art of the description of process 2 at low momentum transfer. In order to extend the theoretical description of the two-nucleon emission processes to the high momentum transfer region, where three-body continuum Faddeev-like wave functions are not yet available, we have developed an approach to the three-body rescattering, to be presented in the next subsection, based upon the eikonal approximation, which not only allows one to calculate the high momentum transfer processes, but can also easily be extended to complex nuclei.

C. Three-body rescattering

We have considered the three-body rescattering of the neutron with the interacting pp pair within an extended Glauber-type approach [28] based on the following assumption:

$$\chi_{(1/2)\sigma_n} \exp(-i\mathbf{p}_n\mathbf{r}_3) \Psi^{\mathbf{p}_{rel}}_{S_{pp}\Sigma_{pp}}(\mathbf{r}_1,\mathbf{r}_2)$$

$$\rightarrow \hat{G}(\mathbf{r}_1,\mathbf{r}_2,\mathbf{r}_3)\chi_{(1/2)\sigma_n} \exp(-i\mathbf{p}_n\mathbf{r}_3) \Psi^{\mathbf{p}_{rel}}_{S_{pp}\Sigma_{pp}}(\mathbf{r}_1,\mathbf{r}_2),$$

(33)

where the Glauber operator $\hat{G}$ is [29]

$$\hat{G}(\mathbf{r}_1,\mathbf{r}_2,\mathbf{r}_3) = \prod_{i=1}^{2} [1 - \theta(z_i - z_3)\Gamma(\mathbf{b}_i - \mathbf{b}_3)], \quad (34)$$

with $\mathbf{b}_i$ and z_i being the transverse and the longitudinal coordinates of the nucleon, and $\Gamma(\mathbf{b})$ the profile function of the elastic nucleon-nucleon scattering amplitude; for the latter, the standard high-energy parametrization, viz.,

$$\Gamma(\mathbf{b}) = \frac{\sigma^{tot}_{NN}(1 - i\alpha_{NN})}{4\pi b_0^2} \exp\left(-\frac{b^2}{2b_0^2}\right), \quad (35)$$

has been used, where σ^{tot}_{NN} is the total nucleon-nucleon (NN) cross section and α_{NN} the ratio of the imaginary to the real part of the NN scattering amplitude. Within such an approach, the full distorted transition matrix element assumes the following form:

$$M^D(\mathbf{p}_m, \mathbf{p}_{rel})$$

$$= \frac{1}{2} \sum_{\mathcal{M}} \sum_{S_{pp}, \Sigma_{pp}} \sum_{\sigma_n} |T^D(\mathcal{M}, \sigma_n, S_{pp}, \Sigma_{pp}, \mathbf{p}_m, \mathbf{p}_{rel})|^2,$$

(36)

where

$$\mathbf{p}_m = \mathbf{p}_n - \mathbf{q} = -(\mathbf{p}_1 + \mathbf{p}_2) \quad (37)$$

is the *missing momentum*, which coincides with the neutron momentum before interaction when the three-body rescattering is disregarded. The distorted scattering matrix T^D has the form

$$T^D(\mathcal{M}, \sigma_n, S_{pp}, \Sigma_{pp}, \mathbf{p}_n, \mathbf{p}_{rel})$$

$$= \frac{2}{\pi} \int \tilde{t}^2 d\tilde{t} d^3\rho d^3r \exp(-i\mathbf{p}_m\boldsymbol{\rho}) \Omega^{\tilde{t},\mathbf{p}_{rel}}_{\mathcal{M},\sigma_n,S_{pp},\Sigma_{pp}}(\mathbf{r},\boldsymbol{\rho}),$$

(38)

with

$$\Omega^{\tilde{t},t}_{\mathcal{M},\sigma_n,S_{pp},\Sigma_{pp}}(\mathbf{r},\boldsymbol{\rho})$$

$$= \sum_{\{\alpha\}} \langle XM_X L_\rho M_\rho | \tfrac{1}{2}\mathcal{M}\rangle \langle j_{12} M_{12} \tfrac{1}{2}\sigma_n | XM_X\rangle$$

$$\times \langle l_f m_f S_{pp} \Sigma_{pp} | j_f M_f\rangle Y_{l_f m_f}(\hat{\mathbf{p}}_{rel}) Y_{L_\rho M_\rho}(\hat{\boldsymbol{\rho}}) I^{[\tilde{t}]}_{\{\alpha\}}(|\boldsymbol{\rho}|)$$

$$\times [R^{j_f,t}_{l_f S_{pp}}(r) R^{j_{12},\tilde{t}}_{l_{12}S_{pp}}(r)][Y^{j_{12}M_{12}}_{l_{12}S}(\hat{\mathbf{r}}) Y^{*j_f M_f}_{l_f S_f}(\hat{\mathbf{r}})]\hat{G}(\mathbf{r},\boldsymbol{\rho}),$$

$$(39)$$

and the response is given by Eq. (21), with $M^{pp}(\mathbf{p}_n,\mathbf{p}_{rel})$ replaced by $M^D(\mathbf{p}_n,\mathbf{p}_{rel})$ [31].

Some details of our numerical calculations of the three-body rescattering transition form factor, Eq. (38), are now in order. It can be seen that the dependence of $T^D(\mathcal{M},\sigma_n,S_{pp},\Sigma_{pp},\mathbf{p}_n,\mathbf{p}_{rel})$ upon $\mathbf{p}_{rel}$ is entirely governed by the quantity $\Omega^{\tilde{t},t}_{\mathcal{M},\sigma_n,S_{pp},\Sigma_{pp}}(\mathbf{r},\boldsymbol{\rho})$. Since the main component of the ³He ground-state wave function corresponds to the relative motion of the pp pair in the ^1S_o wave, the two protons in the final state are mostly in states with spin $S=0$ and even values of the relative angular momenta; thus $\Omega^{\tilde{t},t}_{\mathcal{M},\sigma_n,S_{pp},\Sigma_{pp}}(\mathbf{r},\boldsymbol{\rho})$ is almost symmetric under the exchange $\mathbf{t}\leftrightarrow-\mathbf{t}$. This symmetry can be slightly violated due to the contribution of the highest partial pp waves in the ³He wave function [29].

The quantities σ^{NN}_{NN}, α_{NN} and b_0 in Eq. (35) depend in principle on the total energy of the interacting nucleons [28], however, at high values of $|\mathbf{p}_n|$ ($|\mathbf{p}_n|\gtrsim 0.7$ GeV/c, which implies high values of the momentum transfer $|\mathbf{q}|$), they become energy independent and the "asymptotic" values $\sigma_{tot}(NN) \sim 44$ mb, $\alpha_{NN} \simeq -0.4$ can be used, with b_0 determined by σ^{NN}_{NN} and α_{NN} from unitarity requirements [28].

The transition form factor $M^D(\mathbf{p}_n,\mathbf{p}_{rel})$ is shown Figs. 10–12, where it is compared with M^{PWA} and M^{pp}. The three figures correspond to three different kinematical conditions, namely the following:

(i) Figure 10 shows the results obtained in the superparallel kinematics ($\theta_1=180°$) and $|\mathbf{p}_{rel}|=0.75$ fm^{-1}, vs $|\mathbf{P}|=|\mathbf{p}_1+\mathbf{p}_2|=|\mathbf{p}_n-\mathbf{q}|$. Let us, first of all, discuss the results obtained within the PWA and the PWA plus pp rescattering (dashed and dot-dashed curves, respectively), which obviously coincide with the results presented in Fig. 9 (top panel, $\theta_1=180°$), since $\mathbf{p}_n=\mathbf{k}_n+\mathbf{q}$ and $\mathbf{P}=\mathbf{p}_{mis}=-\mathbf{k}_n$. The arrow denotes the 2NC kinematics, when $\mathbf{k}_1=-\mathbf{k}_n$, $\mathbf{k}_2=0$ ($\mathbf{p}_1+\mathbf{p}_n=\mathbf{q}$, $\mathbf{p}_2=0$) and $|\mathbf{k}_n|=2|\mathbf{p}_{rel}|$. In agreement with Fig. 9, we see that the pp rescattering has large effects at low values of $|\mathbf{P}|=|\mathbf{k}_n|$, but gives negligible contributions when $|\mathbf{P}|=|\mathbf{k}_n|\gtrsim 2|\mathbf{p}_{rel}|=1.5$ fm^{-1}. The full line in Fig. 10 includes the effects from $n-pp$ rescattering (when $\mathbf{p}_m\neq-\mathbf{k}_n$); these effects are very large at small values of $|\mathbf{P}|$, but becomes negligible at $|\mathbf{P}|\gtrsim 2|\mathbf{p}_{rel}|$. One could be tempted to compare the results shown in Fig. 10 with the ones presented in Fig. 5. In this respect one should first of all stress that in the sym kinematics used in Fig. 5, the *neutron* is at rest (both in the initial and final states), which means that the transition matrix element is mainly governed by the $^1S_0$ wave function of
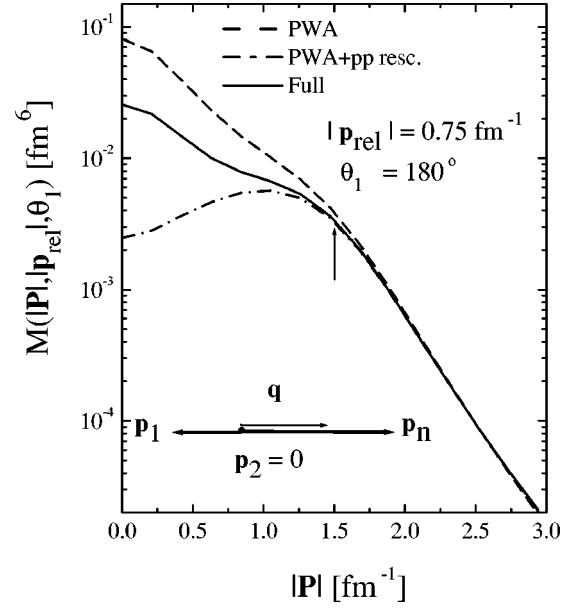

FIG. 10. The transition form factor $M(|\mathbf{P}|,|\mathbf{p}_{rel}|,\theta_1) = M(\mathbf{p}_n,\mathbf{p}_{rel},\mathbf{q})$ [Eq. (10)], plotted vs the two-nucleon center-of-mass (or *missing*) momentum $|\mathbf{P}|=|\mathbf{p}_1+\mathbf{p}_2|=|\mathbf{p}_m|=|\mathbf{q}-\mathbf{p}_n|$ for fixed values of the relative momentum $|\mathbf{p}_{rel}|$ and the angle θ_1 between $\mathbf{q}$ and $\mathbf{p}_{rel}$. The dashed and dot-dashed lines represent, as in Fig. 9, the PWA [Eq. (16)] and the PWA plus pp rescattering [Eq. (10)], respectively, whereas the full line includes also the $n-(pp)$ rescattering according to Eq. (36). The arrow and the momentum vector balance, which refer to the dashed and the dot-dashed lines, denote the point where Eq. (32) is satisfied, i.e., $|\mathbf{k}_n|=2|\mathbf{p}_{rel}| = 1.5$ fm^{-1}, $\mathbf{k}_1=-\mathbf{k}_n$, $\mathbf{k}_2\simeq 0$; when $\theta_1=0°$, the behavior of the dashed and dot-dashed lines is exactly the same, with the arrow denoting in this case the configuration with $|\mathbf{k}_n|=2|\mathbf{p}_{rel}|$, $\mathbf{k}_2\simeq -\mathbf{k}_n$, $\mathbf{k}_1\simeq 0$. The inclusion of the $n-(pp)$ rescattering destroys in principle the $\theta_1=0°-180°$ symmetry, but, as explained in the text, the asymmetry generated by our calculation is very mild. For $|\mathbf{P}|>1.5$ fm^{-1}, the ground-state momentum balance is always similar to the 2NC configuration ($|\mathbf{k}_n|\simeq|\mathbf{k}_1|$, $|\mathbf{k}_2|\ll|\mathbf{k}_1|$), whereas for $|\mathbf{P}|<1.5$ fm^{-1}, the configuration is far from the 2NC one. Three-nucleon wave function from [19]; AV18 interaction [22].

the two-proton relative motion. In the process considered in Fig. 10, when γ^* couples to the neutron, none of the nucleons are at rest, except nucleon 2 in the particular kinematics denoted by the arrow which represents the absorption of γ^* by a neutron of a correlated np pair, with the spectator *proton* at rest both in the initial and the final states. In this case, the transition matrix element gets contributions from higher angular momentum states, whose main effect is to fill in the diffraction minimum, without significantly affecting the regions left and right to it; consequently, in these regions, the value of $M(\mathbf{P},|\mathbf{p}_{rel}|,\theta_1)$ corresponding to the arrow in Fig. 10 (i.e., to a spectator nucleon at rest), can qualitatively be compared with the results shown in Fig. 5 at $\mathbf{p}_{2z}=-\mathbf{p}_{1z}=1.5$ fm^{-1}; in this case one finds indeed that the relative momentum of the np pair is $|\mathbf{p}_{rel}|\simeq 0.75$ fm^{-1}. Thus in Fig. 5 the region where FSI effects are small, correspond to the 2NC region where, moreover, the conditions for the validity of the Schrödinger approach are satisfied. Note that, eventually, according to our Glauber calculation, as well as to the
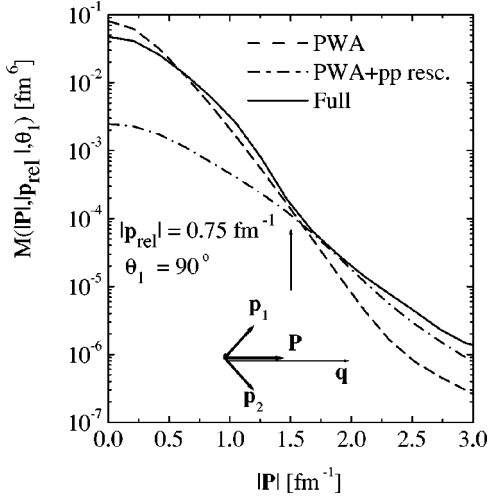
FIG. 11. The same as in Fig. 10 but for $\theta_1 = 90°$ (cf. Fig. 9, as far as the dashed and dot-dashed lines are concerned). The arrow and the momentum vector balance correspond to the point where Eq. (32) is satisfied ($|\mathbf{k}_n| = 2|\mathbf{p}_{rel}| = 1.5$ fm^{-1}), but since $\theta_1 \neq 0°$ (180°), we do not stay now in the *two nucleon correlation* region, but rather in the *three-nucleon correlation* region, for $|\mathbf{k}_2| \simeq |\mathbf{k}_1| \simeq |\mathbf{k}_n|/\sqrt{2} \simeq 1.1$ fm^{-1} (cf. the Appendix). Three-nucleon wave function from Ref. [19]; AV18 interaction [22].

calculation of Ref. [21], the curves shown in Fig. 5 are slightly affected by the pn rescattering; thus the dashed line in Fig. 5 includes effectively both the PWA and pp rescattering results shown in Fig. 10.

(ii) Figure 11 displays the same as in Fig. 10, but for $\theta_1 = 90°$. The dashed and dot-dashed lines are of course the same as in Fig. 9. In particular, at $|\mathbf{k}_n| = 1.5$ fm^{-1}, corresponding to the condition $|\mathbf{k}_n| = 2|\mathbf{p}_{rel}|$, the $n - pp$ rescattering is small. Note that in this case, in spite of the fulfillment
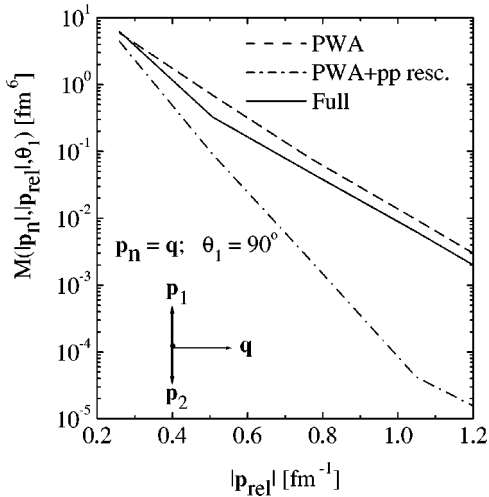

FIG. 12. The transition form factor $M(|\mathbf{P}|, |\mathbf{p}_{rel}|, \theta_1) = M(\mathbf{p}_n, \mathbf{p}_{rel}, \mathbf{q})$ [Eq. (10)], plotted vs $|\mathbf{p}_{rel}|$ for $\mathbf{p}_n = \mathbf{q}$, $\theta_1 = 90°$. The process corresponds to the absorption of γ^* by a neutron at rest followed by the emission of two protons with momenta $\mathbf{p}_1 = -\mathbf{p}_2$ (*back-to-back* protons). Three-nucleon wave function from Ref. [19]; AV18 interaction [22].

of the above condition, we are not in the two-nucleon correlation region but rather in the three-nucleon correlation region, for, as shown in the figure, the momenta of the three-nucleons in the ground state are of comparable size ($|\mathbf{k}_1| \simeq |\mathbf{k}_2| \simeq |\mathbf{k}_n|/\sqrt{2}$, $\theta_{12} \simeq 90°$). Note that in the PWA the transition form factor both in process 1 (interaction of γ^* with a proton of a correlated pp pair shown in Figs. 4 and 5) and process 2 (the interaction of γ^* with the neutron we are discussing), represent the same quantity, namely, the three-body wave function in momentum space [cf. Eqs. (16) and (25)]; therefore the results presented in Figs. 10 and 11 at $|\mathbf{P}| = |\mathbf{k}_n| = 0$ have to coincide with the ones given in Fig. 3 at the corresponding value of $\mathbf{p}_{rel} = \mathbf{k}_{rel}$, as indeed is the case.

(iii) Figure 12 refers to the particular case when the neutron is at rest in the ground state, so that, after absorbing γ^*, it leaves the system with momentum $\mathbf{p}_n = \mathbf{q}$, and the two protons are emitted back to back in the lab system with $|\mathbf{p}_1| = |\mathbf{p}_2|$ and $\theta_1 = 90°$. This is the kinematics also considered in Ref. [14]. Since, as already pointed out [cf. Sec. III B, Eq. (25)], in PWA both process 1 and process 2 are described by the same transition form factor, which is nothing but the momentum space three-body wave function, the dashed lines in Figs. 4 and 12 represent the same quantity. As a matter of fact, since in Fig. 12 $|\mathbf{p}_{rel}| = |\mathbf{p}_2|$, we see that at the highest values of $|\mathbf{p}_{rel}|$ the dashed lines in Fig. 4 and 12 are in agreement; note, however, that, due to the effect of the high angular momentum states, the dashed line in Fig. 12 should not exhibit the diffraction minimum seen in Fig. 4. It can be seen, as expected from the behavior of the neutron spectral function, that the pp rescattering is very large since the ground-state configuration corresponds to zero neutron momentum and large pp relative momentum. The fact that the pp rescattering is large, would not represent *per se* a serious obstacle in the investigation of the three-body spectral function, for, as also stressed in Ref. [14], the calculation of the pp rescattering is well under control since many years (see, e.g., Ref. [23]); unfortunately, also the full rescattering effects are very large, with the results that this kinematics is not the optimal one to investigate the three-body wave function. The results presented in Fig. 12 can qualitatively be compared with the results of Faddeev-like calculations of Ref. [14], bearing in mind that the latter are restricted to low momentum transfer, i.e., to $\sqrt{s} \lesssim 3M + m_\pi$, which means that unlike our case, for a given value of the three-momentum transfer $|\mathbf{q}|$, there is an upper limit to the value of $|\mathbf{p}_{rel}|$. As far as the PWA and pp rescattering results are concerned, there is en excellent agreement between our results and the plane wave impulse approximation antisymmetrized (PWIAS) and "tG_0" results of Ref. [14], respectively, which is not surprising in view of the similarity of the wave functions and the treatment of the two-nucleon spectator rescattering adopted in the two calculations; as for the three-body rescattering contribution, there also appear to be a satisfactory agreement between our eikonal-type calculation and the Faddeev results, provided the values of the three-momentum transfer is large enough; at low values of the momentum transfer the eikonal-type approach cannot be applied and a consistent treatment of bound and continuum

three-nucleon states within the Schrödinger approach is necessary. It should be stressed that in Ref. [14] the effect of the three-body rescattering on the process in which γ^* is absorbed by a proton at rest and the proton and the neutron are emitted back to back with equal momenta $\mathbf{p}_n = -\mathbf{p}_2 \equiv \mathbf{p}$, has been found to be very small, so that this process would be well suited for the investigation of the three-nucleon wave function, being the calculation of the $p-n$ rescattering well under control, as previously pointed out; it should, moreover, be emphasized that within such a kinematics the effect of π and ρ meson exchange contributions on the transverse transition form factor was also found to be very small [14]. However, the sp kinematics at $|\mathbf{p}_m| \gtrsim 2|\mathbf{p}_{rel}|$ we have considered seems to be very promising, in view of the smallness of both the spectator pair and the three-body rescattering contributions.

IV. SUMMARY AND CONCLUSIONS

In this paper we have investigated the effects of the final state interaction (FSI) in the process $^3\mathrm{He}(e,e'2p)n$ using realistic three-nucleon wave functions which, being the exact solution of the Schrödinger equation, incorporate all types of correlations generated by modern NN potentials. We have taken into account FSI effects, treating the three-nucleon rescattering within an improved eikonal approximation, which allows one to consider the two-nucleon emission processes at high momentum transfer, also when $\sqrt{s} \gtrsim 3M + m_\pi$, i.e., above the kinematical boundary imposed by Faddeev-like calculations. We reiterate once again that our aim was restricted to the development of a theoretical approach for the treatment of FSI effects in two-nucleon emission processes off the three-body system, and to the investigation of the effects produced by FSI in various kinematical regions. We did not discuss, other final state effects, e.g., MEC, which clearly have to be taken into account when theoretical predictions are compared with experimental data. We have been guided by the idea that if a kinematical region could be found, where the effects of FSI are minimized, this would represent a crucial advance towards the investigation of both GSC and current operators. Basically we have considered two different mechanisms leading to the two-proton emission process:

(i) *Mechanism 1*, in which γ^* is absorbed by a correlated pp pair. This mechanism, which is the one usually considered in the case of complex nuclei, has been previously analyzed in Ref. [21] within a particular kinematics, the so called *symmetric kinematics*, according to which $\mathbf{p}_1 + \mathbf{p}_2 = \mathbf{q}$, $\mathbf{p}_n = 0$. In PWA, such a kinematics selects the ground-state wave function configuration in which $\mathbf{k}_1 \simeq -\mathbf{k}_2$, $\mathbf{k}_n = 0$ [the *two-nucleon correlation* (2NC) configuration]. Our calculations confirm the results of Ref. [21], namely that the FSI due to the $n-(pp)$ rescattering is very small, whereas the pp rescattering is extremely large, and fully distorts the direct link between the ground-state wave function and the cross section, which holds in PWA (cf. Fig. 4). Thus the symmetric kinematic does not appear extremely useful to investigate the three-nucleon wave function. A more interesting kinematics is the superparallel kinematics ($\mathbf{p}_{1\perp} = \mathbf{p}_{2\perp}$

$=0, p_{1z} + p_{2z} = |\mathbf{q}|, \mathbf{q} \| z$) which, as demonstrated in Fig. 5, shows that, particularly at high values of the momenta of the detected protons, the effects from the FSI are strongly reduced.

(ii) *Mechanism 2*, in which γ^* is absorbed by the neutron, and the two protons are detected. We have shown that if the pp rescattering is taken into account and the one between the neutron and the protons disregarded, the cross section depends upon the *vector spectral function* $\mathcal{P}_1(\mathbf{k}_n, \mathbf{p}_{rel})$ $= (M_N |\mathbf{p}_{rel}|/2) M^{pp}(\mathbf{k}_n, \mathbf{p}_{rel})$. This spectral function, unlike the usual one (see, e.g., Ref. [23]), depends not only upon $|\mathbf{k}_n|$ and $|\mathbf{p}_{rel}| = \sqrt{2ME^*}$, but also upon the angle θ between them. By analyzing the behavior of $\mathcal{P}_1(\mathbf{k}_n, \mathbf{p}_{rel})$ (cf. Fig. 9) we have demonstrated that (i) when the relation $|\mathbf{k}_n|$ $\simeq 2|\mathbf{p}_{rel}|$ holds, the FSI due to pp rescattering is very small, and (ii) the dominant configuration in the ground-state wave function is the 2NC one, in which $\mathbf{k}_1 \simeq -\mathbf{k}_2$, $\mathbf{k}_n = 0$ [Eq. (28)]; we have also found that when $\theta \simeq 0°(180°)$, the smallness of pp rescattering actually extends to a wide region characterized by $|\mathbf{k}_n| > 2|\mathbf{p}_{rel}|$, where the 2NC configuration is still the dominant one (cf. the Appendix). Such a picture is not in principle withstanding when the three-nucleon $n-(pp)$ rescattering is taken into account, since in this case the concept of neutron momentum before interaction $\mathbf{k}_n$ has to be abandoned in favor of the concept of *missing momentum* $\mathbf{p}_m = \mathbf{p}_n - \mathbf{q} = -(\mathbf{p}_1 + \mathbf{p}_2)$, which equals $\mathbf{k}_n$ only when the three-body rescattering is disregarded. However, our consideration of the three-body rescattering, clearly show that in the case of the superparallel kinematics, both the three-body and two-body rescattering are negligible when $|\mathbf{p}_m|$ $\gtrsim 2|\mathbf{p}_{rel}|$, which means that in this region $|\mathbf{p}_m| \simeq |\mathbf{k}_n|$. The three-body rescattering is on the contrary very relevant when $|\mathbf{p}_m| < 2|\mathbf{p}_{rel}|$, both in the case of the superparallel kinematics, and particularly when the two protons are detected with their relative momentum perpendicular to the direction of $\mathbf{q}$ (cf. Fig. 11). Within mechanism 2 we have, as in Ref. [14], also considered the process in which γ^* is absorbed by a neutron at rest and the two protons are emitted back to back in the direction perpendicular to the direction of the momentum transfer $\mathbf{q}$, which means $\mathbf{p}_m = 0$. In this case, the effects from the FSI appear to be very different from the ones considered in the two previous cases, namely, unlike the symmetric kinematics (cf. Figs. 4 and 5), where only the FSI between the two active protons played a substantial role, here *both* the pp rescattering and the three-body $n-(pp)$ rescattering are very large (cf. Fig. 12).

We can summarize the main results we have obtained in the following way:

(i) If γ^* is absorbed by a correlated proton pair, with the spectator neutron at rest and the two protons detected with their relative momentum perpendicular to the direction of $\mathbf{q}$ (symmetric kinematics), the leading FSI is the pp rescattering, with the $n-(pp)$ rescattering playing only a minor role. In such a case, however, the pp rescattering fully destroys the direct link between the ground-state wave function and the cross section, occurring in the PWA; if the protons, on the contrary, are detected with their relative momentum parallel to $\mathbf{q}$ (superparallel kinematics), the effects of the pp

rescattering is appreciably suppressed, particularly at high values of the momenta of the detected protons.

(ii) If γ^* is absorbed by an uncorrelated neutron at rest and the two correlated protons are emitted back to back with $\mathbf{p}_1 = -\mathbf{p}_2$, $\mathbf{p}_{rel} = \mathbf{p}_1 \perp \mathbf{q}$, *both* the pp and the $n-(pp)$ rescattering are very large.

(iii) If γ^* is absorbed by a neutron and the two protons are detected in the superparallel kinematics, one has the following situation: if $|\mathbf{p}_m| < 2|\mathbf{p}_{rel}|$ *both* the pp and the $n-(pp)$ rescattering are large; if, on the contrary, $|\mathbf{p}_m| \geqslant 2|\mathbf{p}_{rel}|$ they are both small and the cross section can be directly linked to the three-body wave function in momentum space.

In conclusion it appears that the superparallel kinematics with $|\mathbf{p}_m| \geqslant 2|\mathbf{p}_{rel}|$ could represent a powerful tool to investigate the structure of the three-body wave function in momentum space. Experimental data in this kinematical region would be therefore highly desirable.

APPENDIX: BASIC CONFIGURATIONS IN THE VECTOR SPECTRAL FUNCTION

Let us investigate the basic configuration in the vector spectral function. To this end, we will first consider the three-body wave function in momentum space or, in other words, the vector spectral function in the plane wave approximation, when the momenta of the three-nucleons satisfy the relation

$$\mathbf{k}_1 + \mathbf{k}_2 + \mathbf{k}_n = 0, \tag{A1}$$

i.e.,

$$\mathbf{k}_{1(2)} = -\frac{1}{2}\mathbf{k}_n \pm \mathbf{k}_{rel}, \tag{A2}$$

where $\mathbf{k}_{rel} = (\mathbf{k}_1 - \mathbf{k}_2)/2$ is the relative momentum. One thus has

$$|\mathbf{k}_{1(2)}| = \sqrt{\mathbf{k}_{rel}^2 + \frac{\mathbf{k}_n^2}{4} \mp |\mathbf{k}_{rel}||\mathbf{k}_n|\cos\theta}. \tag{A3}$$

The above relation illustrates that:

(i) If $|\mathbf{k}_n| = 2|\mathbf{k}_{rel}|$, $|\mathbf{k}_1| = 0$, $\mathbf{k}_n = -\mathbf{k}_2$, when $\theta = 0°$, and $|\mathbf{k}_2| = 0$, $\mathbf{k}_n = -\mathbf{k}_1$, when $\theta = 180°$, which represents the two-nucleon correlation (2NC) configuration. It should be pointed out that the scalar condition $|\mathbf{k}_n| = 2|\mathbf{k}_{rel}|$ alone does not suffice to uniquely specify the ground-state configuration, in particular the 2NC configuration. As a matter of fact, when $|\mathbf{k}_n| = 2|\mathbf{k}_{rel}|$ but $\theta = 90°$, one has $|\mathbf{k}_1| = |\mathbf{k}_2| = \sqrt{2}|\mathbf{k}_{rel}|$ which represents a typical three-nucleon correlation (3NC) configuration, for all of the three-nucleons have comparable and high momenta. However, it can be seen from Fig. 9 that such a three-nucleon configuration is strongly suppressed, and $P(k_n, E)$ is mainly governed by the 2NC configuration.

(ii) If $|\mathbf{k}_n| \neq 2|\mathbf{k}_{rel}|$, we do not stay in the 2NC configuration, but it can easily be checked that if $|\mathbf{k}_n| > 2|\mathbf{k}_{rel}|$ and $\theta \simeq 0°(180°)$, $|\mathbf{k}_n|$ is still comparable with $|\mathbf{k}_{2(1)}| \gg |\mathbf{k}_{1(2)}|$.

The above picture is distorted by the pp rescattering, but, as demonstrated in Fig. 9, only for (i) $|\mathbf{k}_n| < 2|\mathbf{k}_{rel}|$ and (ii) $|\mathbf{k}_n| > 2|\mathbf{k}_{rel}|$, $\theta \simeq 90°$.

[1] W. Glöckle, H. Witala, D. Huber, H. Kamada, and J. Golak, Phys. Rep. **274**, 107 (1996).

[2] J. Carlson and R. Schiavilla, Rev. Mod. Phys. **70**, 743 (1998).

[3] S. C. Pieper and R. B. Wiringa, Rev. Mod. Phys. **51**, 53 (2001).

[4] S. Boffi, C. Giusti, and F. D. Pacati, Phys. Rep. **226**, 1 (1993).

[5] C. Giusti and F. D. Pacati, Nucl. Phys. **A535**, 573 (1991).

[6] T. Emura et al., Phys. Rev. Lett. **73**, 404 (1994).

[7] P. Grabmayr, in *Proceedings of the Third International Conference on Perspectives in Hadronic Physics*, edited by S. Boffi, C. Ciofi degli Atti, and M. Giannini [Nucl. Phys. **A699**, 41c (2002)].

[8] C. Giusti, F. D. Pacati, K. Allaart, W. J. W. Geurts, W. H. Dickhoff, and H. Muther, Phys. Rev. C **57**, 1691 (1998).

[9] J. Ryckebusch et al., Nucl. Phys. **A624**, 581 (1997); G. Rosner, in *Proceedings of the Conference on Perspectives in Hadronic Physics*, edited by S. Boffi, C. Ciofi degli Atti, and M. Giannini (ICTP, World Scientific, Singapore, 1997), p. 185.

[10] K. I. Blomqvist et al., Phys. Lett. B **421**, 71 (1998).

[11] C. J. G. Onderwater et al., Phys. Rev. Lett. **78**, 4893 (1997); **81**, 2213 (1998); R. Starink et al., Phys. Lett. B **474**, 33 (2000).

[12] S. Ishikawa et al., Phys. Rev. C **57**, 39 (1998).

[13] A. Kievsky, S. Rosati, and M. Viviani, Nucl. Phys. **A551**, 241 (1993).

[14] J. Golak, H. Kamada, H. Witala, W. Glöckle, and S. Ishikawa, Phys. Rev. C **51**, 1638 (1995); W. Glöckle et al., in *5th Workshop on Electromagnetically Induced Two-Hadron Emission*, Lund, Sweden, June 2001, edited by P. Grabmayr; Acta Phys. Pol. B **32**, 3053 (2001); W. Glöckle (private communication).

[15] D. Groep et al., Phys. Rev. Lett. **83**, 5443 (1999); Phys. Rev. C **63**, 014005 (2001).

[16] K. Egiyan, L. Frankfurt, W. R. Greenberg, G. A. Miller, M. Sargsyan, and M. Strikman, Nucl. Phys. **A580**, 365 (1994).

[17] L. B. Weinstein, in *5th Workshop on Electromagnetically Induced Two-Hadron Emission* (Ref. [14]); (private communication); B. Zhang, W. Bertozzi, and S. Gilad, *ibid*.

[18] C. Ciofi degli Atti and L.P. Kaptari, in *5th Workshop on Electromagnetically Induced Two-Hadron Emission* (Ref. [14]); Nucl. Phys. **A699**, 49c (2002).

[19] A. Kievsky, S. Rosati, and M. Viviani, Phys. Rev. Lett. **82**, 3759 (1999); A. Kievsky (private communication).

[20] A. G. Sitenko, *Scattering Theory* (Springer-Verlag, Berlin, Heidelberg, 1991).

[21] J. M. Laget, Phys. Rev. C **35**, 832 (1987).

[22] R. B. Wiringa, R. A. Smith, and T. L. Ainsworth, Phys. Rev. C **29**, 1207 (1984).

[23] C. Ciofi degli Atti, E. Pace, and G. Salmè, in *Few Body Systems and Electromagnetic Interactions*, Lecture Notes in Physics Vol. 86 (Springer, Berlin, 1978), p. 316; Phys. Rev. C **21**, 805 (1980).

[24] C. Ciofi degli Atti, L. P. Kaptari, and H. Morita (unpublished).

[25] R. V. Reid, Jr., Ann. Phys. (N.Y.) **50**, 411 (1968).

[26] L. L. Frankfurt and M. I. Strikman, Phys. Rep. **160**, 235 (1988).

[27] C. Ciofi degli Atti, S. Simula, L. L. Frankfurt, and M. I. Strikman, Phys. Rev. C **44**, R7 (1991); C. Ciofi degli Atti and S. Simula, *ibid.* **53**, 1689 (1996).

[28] C. Ciofi degli Atti, L. P. Kaptari, and D. Treleani, Phys. Rev. C **63**, 044601 (2001).

[29] A. Bianconi, S. Jeschonnek, N. N. Nikolaev, and B. G. Zakharov, Phys. Lett. B **343**, 13 (1995).

[30] From now on, for *low (high) momentum transfer* we will mean $\sqrt{s}$ *below (above) the pion threshold*.

[31] The quantity $\mathcal{P}_1^D(\mathbf{k}_n,\mathbf{p}_{rel})=M_N|\mathbf{p}_{rel}|M^D(\mathbf{k}_n,\mathbf{p}_{rel})/2$ can be called the *distorted vector spectral function*.